Phosphoinositide 3-kinase regulatory subunit p85α suppresses insulin action via positive regulation of PTEN

Cullen M. Taniguchi*, Thien T. Tran*, Tatsuya Kondo†, Ji Luo‡§, Kohjiro Ueki¶, Lewis C. Cantley‡§‖, and C. Ronald Kahn*,

*Cellular and Molecular Physiology, Joslin Diabetes Center, Harvard Medical School, Boston, MA 02215; †Department of Metabolic Medicine, Graduate School of Medical Sciences, Kumamoto University, Kumamoto 860-8555, Japan; ‡Department of Systems Biology, Harvard Medical School, Boston, MA 02215; §Division of Signal Transduction, Beth Israel Deaconess Medical Center, Boston, MA 02115; and ¶Department of Metabolic Diseases, Graduate School of Medicine, University of Tokyo, Tokyo 113-0033, Japan

Contributed by Lewis C. Cantley, June 3, 2006

The phosphoinositide 3-kinase (PI3K) pathway is central to the metabolic actions of insulin on liver. Here, we show that mice with a liver-specific deletion of the p85α regulatory subunit of PI3K (L-Pik3r1KO) exhibit a paradoxical improvement of hepatic and peripheral insulin sensitivity. Although PI3K enzymatic activity is diminished in L-Pik3r1KO livers because of a reduced level of regulatory and catalytic subunits of PI3K, insulin-stimulated Akt activity is actually increased. This increased Akt activity correlates with increased phosphatidylinositol (3,4,5)-trisphosphate levels which are due, at least in part, to diminished activity of the (3,4,5)-trisphosphate phosphatase PTEN. Thus, the regulatory subunit p85α is a critical modulator of insulin sensitivity *in vivo* not only because of its effects on PI3K activation, but also as a regulator of PTEN activity.

conditional gene knockout | diabetes | insulin resistance

Insulin action on the liver is required for the proper maintenance of metabolic homeostasis. Under normal conditions, insulin inhibits gluconeogenesis and activates lipogenesis to promote proper fuel utilization in the fed state. The failure of insulin to regulate hepatic function can lead to unfettered hepatic glucose output and elevated lipogenesis in the liver, two key features of the metabolic syndrome (1). Not surprisingly, an overwhelming amount of epidemiological (2) and physiological (3) evidence links hepatic insulin resistance to the development of type 2 diabetes.

The molecular mechanisms that maintain hepatic insulin sensitivity are centered around the class I_A phosphoinositide 3-kinase (PI3K) pathway, which serves a critical node in insulin signaling to its metabolic actions (4, 5). PI3K is an obligate heterodimer with an SH2-containing regulatory subunit (p85) and a catalytic subunit (p110). The regulatory subunit mediates the binding, activation, and localization of the PI3K enzyme (6–8).

Despite the crucial role that the regulatory subunits play in mediating insulin-dependent PI3K signaling, insulin sensitivity correlates inversely with regulatory subunit expression. This paradoxical relationship has been demonstrated by knockouts of the different regulatory subunits. For instance, the deletion of the less abundant isoforms of *Pik3r1* (p55α/p50α) (9) or the minor isoform p85β (10) mildly improve insulin sensitivity, whereas the knockout of the more abundant p85α markedly improves glucose homeostasis (11). Germline deletion of the *Pik3r1* gene and its three products (p85α, p55α, and p50α) also enhances insulin sensitivity, although these mice die perinatally (12). These data indicate that in addition to its traditional positive function as a component of the PI3K holoenzyme, p85α is also a potent negative regulator of insulin signaling.

The negative effects of p85α on insulin action may have important consequences in the pathophysiology of insulin resistance and diabetes. For example, the increased expression of p85α in mouse models of gestational diabetes (13) and in obese humans (14) is strongly linked with insulin resistance. Conversely, heterozygosity for *Pik3r1* prevents the onset of diabetes in genetically insulin-resistant mice (15).

The physiologic and molecular mechanisms that underlie this negative regulation by p85α appear to be complex. At the physiologic level, germline knockouts that delete p85 isoforms in all tissues throughout development cannot discriminate whether the negative action of p85α occurs as a tissue-autonomous effect or as a consequence of altered endocrine communication between insulin-responsive tissues. This situation may also be complicated by potential compensatory adjustments to loss of p85 during development.

To better understand the mechanisms by which p85α regulates insulin sensitivity *in vivo* at the physiologic and molecular level, we created mice with a liver-specific deletion of *Pik3r1* (L-Pik3r1KO). This conditional knockout of *Pik3r1* (p85α, p55α, and p50α) in hepatocytes circumvents the perinatal lethality observed in the corresponding germline knockout mice and furthermore allows us to investigate the specific role of the liver in the physiological actions of p85α. We find that L-Pik3r1KO mice have enhanced hepatic and whole-body insulin sensitivity, as well as increased Akt activity in liver, despite decreased total hepatic PI3K activity. We demonstrate that this negative effect of p85α on insulin sensitivity is due, at least in part, to a role in activation of PTEN lipid phosphatase activity.

Results

L-Pik3r1KO Mice Are Insulin-Sensitive. Mice with a liver-specific deletion of *Pik3r1* were generated via the Cre-loxP system by crossing animals carrying a floxed exon 7, which encodes the N-terminal SH2 domain common to all three transcripts, p85α, p55α, and p50α (16), with mice carrying the *Cre* transgene driven by the albumin promoter (17). The presence of loxP sites in the *Pik3r1* gene did not affect expression of p85α in mice lacking albumin-Cre (16), nor did the presence of albumin-Cre affect p85 expression in mice lacking loxP sites (18). The L-Pik3r1KO mice were born in a normal Mendelian distribution and exhibited normal postnatal growth (data not shown). Western blots of liver extracts of L-Pik3r1KO mice revealed an 80–90% decrease in

Conflict of interest statement: No conflicts declared.

Freely available online through the PNAS open access option.

Abbreviations: HGP, hepatic glucose production; PI3K, phosphoinositide 3-kinase; PIP_3, phosphatidylinositol (3,4,5)-trisphosphate; pTyr, phosphotyrosine.

‖To whom correspondence may be addressed. E-mail: lcantley@hms.harvard.edu.

**To whom correspondence may be addressed at: Joslin Diabetes Center, One Joslin Place, Boston, MA 02215. E-mail: c.ronald.kahn@joslin.harvard.edu.

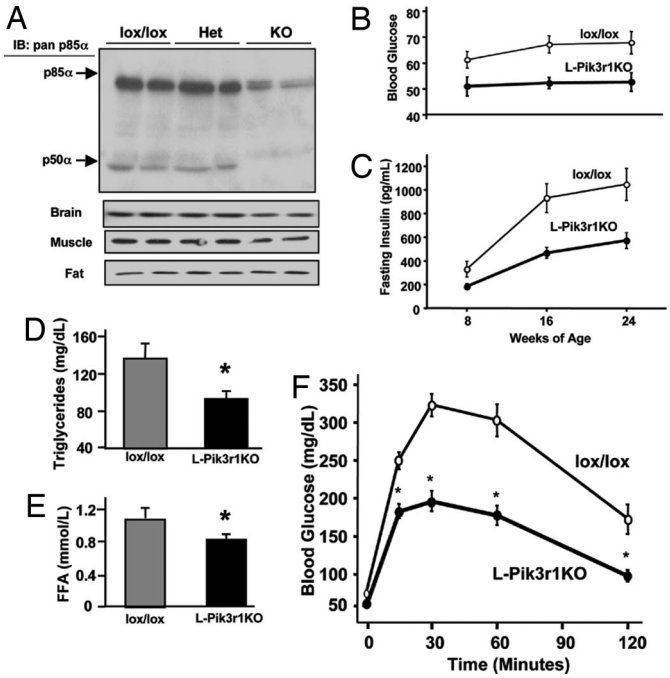

Fig. 1. Metabolic phenotype of L-Pik3r1KO mice. (*A*) Western blots for *Pik3r1* gene products with an antibody against the N-terminal SH2 domain (pan-p85) in tissue lysates, as indicated, from control, heterozygous KO, and L-Pik3r1KO mice. Tissues were collected from mice after an overnight fast, and proteins were extracted and processed as described in *Materials and Methods*. Each lane represents lysates from a different mouse. (*B* and *C*) Fasted blood glucose and fasted serum insulin levels. (*D* and *E*) Serum triglycerides and serum nonesterified free fatty acid (FFA) levels from lox/lox or KO mice in the fasted state. (*F*) Glucose tolerance tests (2 g/kg, i.p.) were performed on mice after a 16-h fast, and blood samples were collected and glucose measured at the times indicated. All values are presented as mean ± SEM ($n = 6–20$). Open circles, lox/lox; filled circles, L-Pik3r1KO.

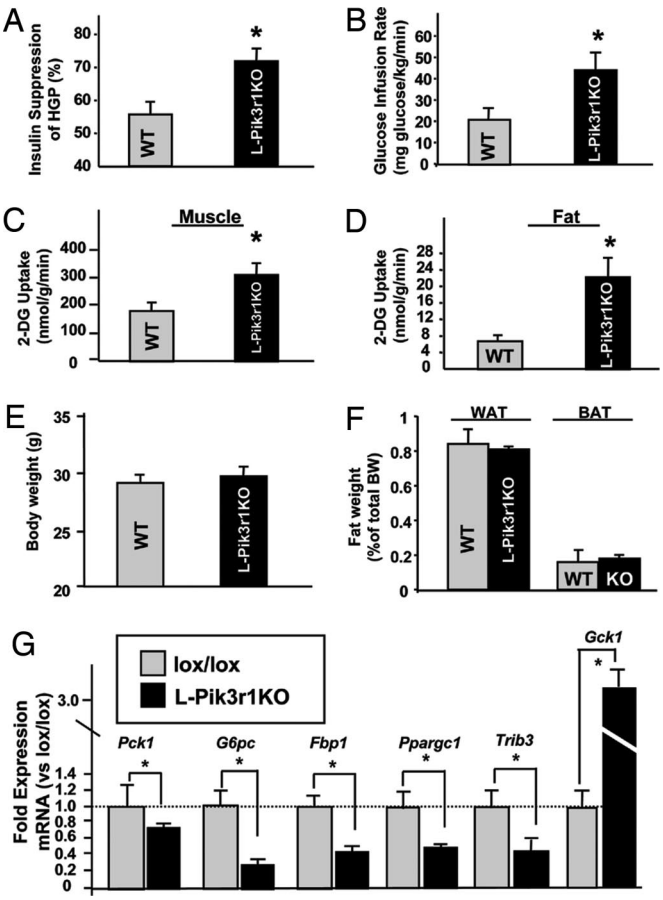

Fig. 2. Hyperinsulinemic–euglycemic clamp analyses and gene expression changes in lox/lox (WT) and L-Pik3r1KO mice. We subjected male mice ($n = 11$) of the indicated genotype at 10–12 weeks of age to hyperinsulinemic–euglycemic clamp analysis and measured insulin suppression of HGP (*A*), glucose infusion rates (*B*), and *in vivo* ^{14}C-deoxyglucose uptake in muscle (*C*) and epididymal fat tissue (*D*). (*E* and *F*) Weight of entire animals or of epididymal (WAT) and brown (BAT) fat pads. WAT and BAT are expressed as a percentage of body weight. (*G*) Quantitative RT-PCR analysis of mRNA levels in lox/lox and L-Pik3r1KO mice of phosphoenolpyruvate carboxykinase (*Pck1*), glucose-6-phosphatase (*G6Pc*), fructose-1,6-bisphosphatase (*Fbp1*), peroxisome proliferator-activated receptor (PPAR) γ coactivator 1α (*Ppargc1*), tribbles3 (*trib3*), and glucokinase (*Gck1*). $n = 8$ for each genotype for RT-PCR experiments. *, $P < 0.05$ vs. lox/lox mice.

p85α and a complete loss of p50α (Fig. 1*A*), consistent with complete ablation in hepatocytes. The remaining p85α is likely due to nonhepatocytes in the liver that express p85α but not p50α. The expression of p85α was unaltered in brain, skeletal muscle, and fat.

Despite the lack of p85α and p50α in liver, L-Pik3r1KO mice exhibited significant improvements in serum metabolic chemistries. Compared with littermate lox/lox controls, L-Pik3r1KO mice displayed lower fasted blood glucose and fasted serum insulin levels at 8, 16, and 24 weeks of age (Fig. 1 *B* and *C*). In addition, L-Pik3r1KO mice exhibited decreased levels of serum triglycerides and circulating free fatty acids (Figs. 1 *D* and *E*). At 16 weeks of age, L-Pik3r1KO mice were significantly more glucose tolerant to an i.p. glucose challenge than controls (Fig. 1*F*). This improved glucose tolerance was observed as early as 8 weeks of age and was maintained through 24 weeks of age (Fig. 5, which is published as supporting information on the PNAS web site).

To further quantify this insulin sensitivity and to determine which tissues were involved in the phenotype, L-Pik3r1KO mice were subjected to a euglycemic–hyperinsulinemic clamp. This revealed increased hepatic insulin sensitivity such that hepatic glucose production (HGP) was suppressed by 25% more in the L-Pik3r1KO mice compared with controls (Fig. 2*A*). Somewhat surprisingly, L-Pik3r1KO mice also displayed improved peripheral insulin sensitivity, as indicated by a 2-fold increase in glucose infusion rates (Fig. 2*B*). This correlated with a 1.5-fold increase in 2-deoxyglucose uptake in muscle (Fig. 2*C*) and a 3-fold increase in 2-deoxyglucose uptake in fat (Fig. 2*D*). Thus, improving insulin sensitivity in the liver secondarily improved insulin sensitivity in peripheral tissues. These improvements in peripheral insulin sensitivity cannot be explained by differences in body weight (Fig. 2*E*) or fat pad size (Fig. 2*F*).

The physiologic data indicating increased hepatic insulin sensitivity corresponded with decreased expression of several key gluconeogenic genes. Quantitative RT-PCR analysis found a decrease in phosphoenolpyruvate carboxykinase (*Pck1*), glucose-6 phosphatase (*G6pc*), and fructose-1,6-bisphosphatase (*Fbp1*) mRNAs in liver by 30%, 70%, and 60%, respectively (Fig. 2*G*). The mRNA levels of the gluconeogenic regulators, peroxisome proliferator-activated receptor (PPAR) γ coactivator 1α (*Ppargc1a*) and tribbles3 (*Trb3*), were also decreased by 50% and 60%, respectively, whereas glucokinase was up-regulated 3-fold. These changes in gene expression were consistent with the notion that the loss of *Pik3r1* in the liver improves hepatic insulin sensitivity.

L-Pik3r1KO Mice Display Significantly Improved Activation of Akt Despite Reduced Total PI3K Activity. To determine the molecular mechanism of the improved insulin sensitivity, we first charac-

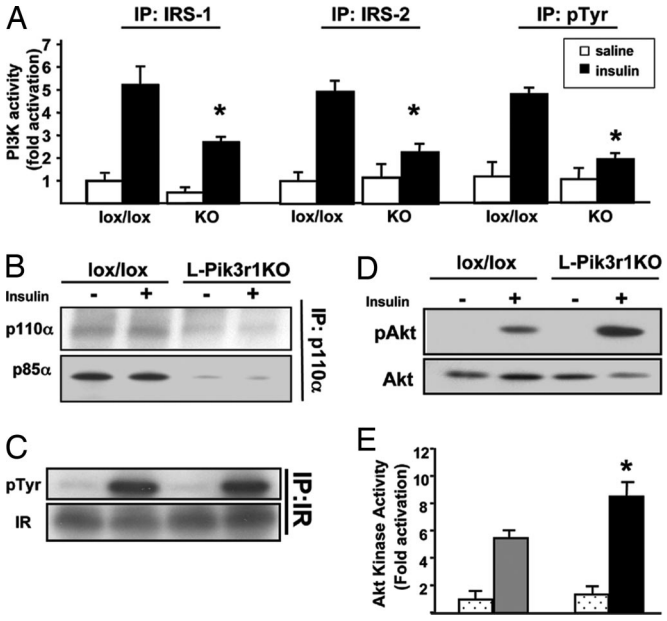

Fig. 3. Enhanced Akt activation in L-Pik3r1KO mice. (*A*) PI3K activity in IRS-1, IRS-2, and pTyr immunoprecipitates (bars represent mean ± SEM; $n = 5$; *, $P < 0.05$). (*B* and *C*) Western blot of p110α and p85α from p110α immunoprecipitates and pTyr and insulin receptor (IR) blots from insulin receptor (β-subunit) immunoprecipitates. (*D*) Ser-473 phosphorylation of Akt (*Upper*) and Akt kinase activity as measured from Akt immunoprecipitates by using Crosstide as a substrate (*Lower*). Bars represent mean ± SEM; $n = 8$; *, $P < 0.05$ vs. insulin-stimulated lox/lox mice.

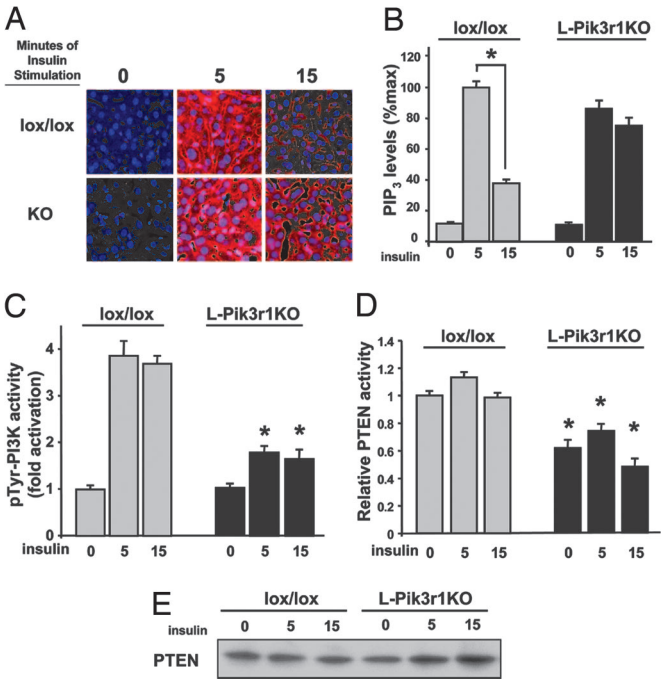

Fig. 4. Enhanced PIP_3 levels in L-Pik3r1KO mice due to decreased PTEN activity. (*A*) Immunofluorescent staining with a primary anti-PIP_3 antibody (IgM) and an anti-mouse secondary antibody conjugated to Alexa Fluor red and counterstained with DAPI. After an overnight fast, mice were injected with saline (time = 0) or 5 units of insulin for the indicated amount of time. Six mice of each genotype/treatment were fixed via cardiac perfusion of 10% buffered formalin in PBS. (*B*) Quantification of the immunofluorescence from PIP_3 staining. Representative slides were chosen from each mouse, and the fluorescence intensity was measured and analyzed with VH-H1A5 ANALYZER software (KEYENCE, Osaka, Japan). (*C* and *D*) Insulin-stimulated pTyr-associated PI3K activity and PTEN activity and PTEN protein levels in lox/lox or KO animals at the indicated time points after insulin stimulation. *, $P < 0.05$ vs. lox/lox after 5 min of insulin stimulation.

terized PI3K function in L-Pik3r1KO mice. As expected, we observed a 50% decrease in IRS-1-associated PI3K activity and a 60% decrease in IRS-2-associated PI3K activity, which together resulted in a 50% reduction in total PI3K activity, as measured from anti-phosphotyrosine (pTyr) immunoprecipitates (Fig. 3*A*). These decreases in PI3K were in part due to the decrease in regulatory subunits but also to the concordant 70% decrease in the expression of the p110α catalytic subunit (Fig. 3*B*) with no change in insulin receptor activation in the L-Pik3r1KO mice (Fig. 3*C*). The decrease in p110α protein levels was expected, because the regulatory subunits are known to stabilize the catalytic subunit (19). Surprisingly, despite these decreases in IRS-1, IRS-2, and pTyr-associated PI3K activity, the activity of Akt was up-regulated by 1.5-fold (Fig. 3*E*), as measured by both Ser-473 phosphorylation and *in vitro* kinase activity of Akt immunoprecipitated from L-Pik3r1KO mice.

Akt is activated by the lipid product of PI3K, phosphatidylinositol (3,4,5)-trisphosphate (PIP_3). To determine whether changes in PIP_3 levels might help to explain the increased Akt activation, we used an immunofluorescent histology technique with an anti-PIP_3 antibody to estimate the accumulation of PIP_3 levels *in vivo* (Fig. 4*A*) (20). After 5 min of insulin stimulation, PIP_3 levels increased ≈10-fold in both control and KO mice. However, after 15 min of stimulation, PIP_3 levels in the L-Pik3r1KO remained high at 74 ± 3.3% of maximum stimulation, whereas PIP_3 levels in the control decreased to 37.7 ± 2.5% of peak levels (Fig. 4*B*). Thus, although less PI3K is associated with IRS proteins in the Pik3r1KO livers, more PIP_3 accumulates over time.

To determine whether this increased accumulation of PIP_3 is due to enhanced PI3K activity or decreased turnover, we directly assessed total PI3K activity and the activity of the lipid phosphatase and tensin homolog (PTEN), which degrades the PIP_3 formed by PI3K (21). Liver pTyr-associated PI3K activity was sustained between 5 and 15 min after insulin stimulation in both the lox/lox and L-Pik3r1KO mice, although the insulin-stimulated PI3K activity of the knockout mice remained at only half the level of the controls because of the reduced regulator and catalytic subunits (Fig. 4*C*). At the same time, the lipid phosphatase activity of PTEN was also consistently decreased by 40% in L-Pik3r1KO at all time points (Fig. 4*D*). Insulin had no effect on the level of PTEN activity in either the control or knockout mice. This decrease in PTEN activity was not due to decreased PTEN expression (Fig. 4*E*) but appeared to be a consequence of reduced hepatic levels of p85.

Discussion

Hepatic insulin signaling is a critical component in the maintenance of whole-body glucose homeostasis, and PI3K signaling plays a key role in liver insulin signaling. We have demonstrated recently that complete ablation of class IA PI3K signaling in the liver through the double deletion of the *Pik3r1* and the *Pik3r2* genes leads to loss of hepatic insulin action, unregulated gluconeogenesis, and diabetes in mice (20). In stark contrast, the selective ablation of only the *Pik3r1* gene in the liver significantly improved hepatic and peripheral insulin sensitivity. This improved insulin sensitivity was demonstrated at the physiologic level with improved glucose tolerance and increased insulin sensitivity, and we further show that the loss of the p85α causes improved Akt activation at the molecular levels because of, in part, the decreased activity of PTEN.

The phenotype of the L-Pik3r1KO mouse sheds light on the physiological mechanisms by which p85 negatively regulates

insulin action *in vivo*. Our data strongly suggest that p85 negatively regulates insulin sensitivity primarily by tempering insulin action in the liver. We infer this from the fact that the phenotype of L-Pik3r1KO mice recapitulates nearly all of the metabolic improvements in glucose tolerance and whole-body insulin sensitivity of other global knockouts of the regulatory subunit of PI3K (11, 12). The deletion of hepatic *Pik3r1* not only enhanced insulin action in liver by directly potentiating PI3K signaling downstream of the insulin receptor, but the loss of p85 also improved insulin sensitivity in other tissues, such as muscle and fat. The enhanced actions of insulin in the periphery in addition to the improved insulin sensitivity in liver probably contributed indirectly to the increased HGP suppression by decreasing the availability of free fatty acids and other gluconeogenic substrates in the blood (22). It is also possible that decreased nutrient delivery to the central nervous system may be playing a role in this phenotype, given the critical role of the hypothalamus in regulating HGP (23). However, taken together, our data supports the notion that hepatic insulin sensitivity is critical to the regulation of whole-body insulin sensitivity (18, 24).

On the surface, these improvements in insulin action appear paradoxical because the ablation of *Pik3r1* led to severe deficiencies in PI3K activation due to the reduction in p85-mediated PI3K activation. For instance, L-Pik3r1KO mice showed a 60% decrease in total hepatic PI3K activity (see Fig. 3 *A* and *E*). However, despite these substantial defects in PI3K function, the activation of Akt downstream of PI3K was not only intact, but enhanced 1.5-fold (Fig. 3*E*).

At the molecular level, the apparent paradox of the improved insulin action afforded by p85 deletion can be attributed to its ability to inhibit PI3K signaling downstream of the insulin receptor. Previously it has been shown that monomeric p85 could inhibit PIP_3 production by competing with PI3K heterodimer for binding to IRS proteins (25) or by altering the subcellular localization of the PI3K signaling complexes (26, 27), thereby preventing the localization of PI3K where its substrate, PI-4,5-P_2, resides. In the present study, we demonstrate that in the liver p85 also regulates, either directly or indirectly, the activity of PTEN *in vivo*. L-Pik3r1KO mice displayed sustained PIP_3 levels during prolonged insulin stimulation (Fig. 4*A*). PIP_3 levels were also elevated in germline p85α-only knockout mice, but it was unclear whether the increase was due to an attenuation of PIP_3 turnover or increased kinase activity (11). The authors of that study attributed the elevated PIP_3 levels to the up-regulation of the short isoforms, p55α and p50α. This mechanism, however, cannot account for the elevated PIP_3 levels observed in L-Pik3r1KO mice because deletion of *Pik3r1* ablates both p55α and p50α in addition to p85α. Although it is not clear how p85α regulates PTEN activity, the mechanism is not likely linked to changes in PTEN expression because L-Pik3r1KO mice showed normal levels of PTEN protein. Although we have not been able to coimmunoprecipitate p85 and PTEN in liver lysates (C.M.T. and C.R.K., unpublished data), others have found p85 as part of a PTEN activating complex in cell lines (28). It thus seems likely that p85α enhances PTEN function by modulating some post-translational modification or altering its subcellular localization.

Our data demonstrate that the p85 regulatory subunit of PI3K has a unique role in insulin signaling and the physiologic regulation of glucose homeostasis. On one hand, p85 mediates PI3K activation through being the obligatory regulatory subunit of p110. However, p85 also plays a novel role in activating negative regulators of the PI3K pathway, particularly the lipid phosphatase PTEN. These mechanisms provide an internal negative feedback on this critical node in insulin and growth factor signaling that could lead to new insights in the disease mechanisms of both type 2 diabetes and cancer (29), as well as basic mechanisms of cell growth and metabolism.

Materials and Methods

Animal Studies. All animals were housed on a 12-h light/12-h dark cycle and fed a standard rodent chow. All protocols for animal use and euthanasia were approved by the Animal Care and Use Committee of the Joslin Diabetes Center and Harvard Medical School in accordance with National Institutes of Health guidelines. All mice in this study were on a 129Sv-C57BL/6-FVB mixed genetic background.

Metabolic Studies. For glucose tolerance testing, blood samples were obtained at 0, 15, 30, 60, and 120 min after i.p. injection of 2 g/kg dextrose. Insulin tolerance tests were performed by injecting 1 unit/kg insulin (Novolin; Novo Nordisk) i.p., followed by blood collection at 0, 15, 30, and 60 min after injection. Blood glucose values were determined by using a OneTouch II glucose monitor (LifeScan). Plasma insulin levels were measured by ELISA with mouse insulin as a standard (Crystal Chem). Nonesterified free fatty acid levels were measured from random fed mice by using a kit from Wako Diagnostics, and serum triglycerides were measured by AniLytics.

Hyperinsulinemic–Euglycemic Clamp. Mice were anesthetized with a 1.2% solution of 2,2,2-tribromoethanol in normal saline, followed by the microsurgical insertion of a catheter into the right jugular vein. After 7–10 days of recovery, mice were fasted for 5 h and infused with a constant dose of insulin (2.5 milliunits/kg/min) and a variable glucose infusion rate to maintain euglycemia and assess whole-body insulin sensitivity (30). An infusion of a [3-^{3}H] glucose tracer was used to ascertain HGP, and a bolus of 2-deoxy-D-[1-^{14}C] glucose was administered during steady-state conditions to determine fat and muscle-specific glucose uptake.

***In Vivo* Insulin Signaling and PIP_3 Quantitation.** After an overnight fast, the mice were anesthetized and injected with 5 units of regular human insulin (Novolin; Novo Nordisk) via the inferior vena cava. Five minutes later, tissues were removed and frozen in liquid nitrogen. Immunoprecipitation and immunoblot analysis of insulin signaling molecules were performed as described in ref. 31. PIP_3 levels were measured by using a monoclonal antibody (IgM; Echelon Biosciences) as described in ref. 20.

Quantitative RT-PCR Analysis. Total RNA was isolated from mouse tissues by using an RNeasy kit (Qiagen), and cDNA was prepared by using the Advantage RT-PCR kit (BD Biosciences) with random hexamer primers, according to the manufacturer's instructions. Ct analysis was performed as described in ref. 31, and the results were expressed as a fold change of mRNA compared with control lox/lox mice.

Antibodies. Rabbit polyclonal anti-IRS-1 antibody (IRS-1), anti-IRS-2 antibody (IRS-2), anti-IR antibody (IR), and pan-p85α antibody were generated as described in ref. 10. Rabbit polyclonal anti-Akt, anti-phospho Akt (S473), and anti-PTEN (for Western blotting) were purchased from Cell Signaling Technology. The pTyr antibody, 4G10, and the PTEN antibody (for immunoprecipitation) were purchased from Upstate Biotechnology. Goat polyclonal anti-Akt1/2 antibody (Akt immunoprecipitation for kinase assay) was purchased from Santa Cruz Biotechnology.

***In Vitro* Kinase Assays.** Tissue homogenates from liver were extracted with tissue homogenization buffer and subjected to immunoprecipitation with IRS-1, IRS-2, or pTyr antibodies followed by PI3K assay as described in ref. 31. For Akt kinase activity, the enzyme was immunoprecipitated from lysates with

a goat polyclonal Akt1/2 antibody, and kinase activity was measured by using Crosstide (Upstate) as a substrate.

PTEN Activity Assay. Phosphatidylinositol (Avanti Polar Lipids) was *in vitro*-phosphorylated to form phosphatidylinositol 3-phosphate (PI-3-P) by recombinant PI3K (Upstate) with [γ-^{32}P]ATP. The phosphorylated lipid was extracted with 1:1 methanol:chloroform, dried under nitrogen gas, reconstituted into PTEN assay buffer (10 mM Tris·HCl/25 mM NaCl, pH 7.5), and incubated with PTEN immunoprecipitates from lox/lox or L-Pik3r1KO liver lysates (32). The PI-3-P was re-extracted with methanol/chloroform and run on a TLC plate with *n*-propanol:2 M acetic acid (65:35). The intensities of PI-3-P spots were quantified with NIH IMAGE (http://rsb.info.nih.gov/nih-image). PTEN activity was determined by decreased intensity of the PI-3-P spot relative to IgG immunoprecipitates from lox/lox livers. Relative PTEN activity was determined by normalizing PTEN activity to lox/lox livers without insulin stimulation.

Statistics. Data are presented as ±SEM. Student's *t* test was used for statistical analysis between two groups, and statistical significance between multiple treatment groups was determined by using ANOVA and Tukey's *t* test.

We thank Laureen Mazzola, Will Wisdom, and Michael Rourk for technical assistance. This work was supported by National Institutes of Health Grants DK33201, DK55545, GM41890 (to L.C.C.), and CA089021 (to L.C.C.) and Joslin Diabetes and Endocrinology Research Center Grant DK34834 (to C.R.K.). C.M.T. acknowledges support from the American Diabetes Association Medical Scholars Award and a Medical Scientist Training Program Scholarship (Harvard Medical School). J.L. acknowledges support from a Howard Hughes Medical Institute Predoctoral Fellowship.

1. Shimomura, I., Matsuda, M., Hammer, R. E., Bashmakov, Y., Brown, M. S. & Goldstein, J. L. (2000) *Mol. Cell* **6,** 77–86.
2. Tripathy, D., Eriksson, K. F., Orho-Melander, M., Fredriksson, J., Ahlqvist, G. & Groop, L. (2004) *Diabetologia* **47,** 782–793.
3. Fisher, S. J. & Kahn, C. R. (2003) *J. Clin. Invest.* **111,** 463–468.
4. Saltiel, A. R. & Kahn, C. R. (2001) *Nature* **414,** 799–806.
5. Taniguchi, C. M., Emanuelli, B. & Kahn, C. R. (2006) *Nat. Rev. Mol. Cell Biol.* **7,** 85–96.
6. Virkamaki, A., Ueki, K. & Kahn, C. R. (1999) *J. Clin. Invest.* **103,** 931–943.
7. Backer, J. M., Myers, M. G., Jr., Shoelson, S. E., Chin, D. J., Sun, X. J., Miralpeix, M., Hu, P., Margolis, B., Skolnik, E. Y., Schlessinger, J. & White, M. F. (1992) *EMBO J.* **11,** 3469–3479.
8. Fruman, D. A., Cantley, L. C. & Carpenter, C. L. (1996) *Genomics* **37,** 113–121.
9. Chen, D., Mauvais-Jarvis, F., Bluher, M., Fisher, S. J., Jozsi, A., Goodyear, L. J., Ueki, K. & Kahn, C. R. (2004) *Mol. Cell. Biol.* **24,** 320–329.
10. Ueki, K., Yballe, C. M., Brachmann, S. M., Vicent, D., Watt, J. M., Kahn, C. R. & Cantley, L. C. (2002) *Proc. Natl. Acad. Sci. USA* **99,** 419–424.
11. Terauchi, Y., Tsuji, Y., Satoh, S., Minoura, H., Murakami, K., Okuno, A., Inukai, K., Asano, T., Kaburagi, Y., Ueki, K., *et al.* (1999) *Nat. Genet.* **21,** 230–235.
12. Fruman, D. A., Mauvais-Jarvis, F., Pollard, D. A., Yballe, C. M., Brazil, D., Bronson, R. T., Kahn, C. R. & Cantley, L. C. (2000) *Nat. Genet.* **26,** 379–382.
13. Barbour, L. A., Shao, J., Qiao, L., Leitner, W., Anderson, M., Friedman, J. E. & Draznin, B. (2004) *Endocrinology* **145,** 1144–1150.
14. Bandyopadhyay, G. K., Yu, J. G., Ofrecio, J. & Olefsky, J. M. (2005) *Diabetes* **54,** 2351–2359.
15. Mauvais-Jarvis, F., Ueki, K., Fruman, D. A., Hirshman, M. F., Sakamoto, K., Goodyear, L. J., Iannacone, M., Accili, D., Cantley, L. C. & Kahn, C. R. (2002) *J. Clin. Invest.* **109,** 141–149.
16. Luo, J., McMullen, J. R., Sobkiw, C. L., Zhang, L., Dorfman, A. L., Sherwood, M. C., Logsdon, M. N., Horner, J. W., Depinho, R. A., Izumo, S. & Cantley, L. C. (2005) *Mol. Cell. Biol.* **25,** 491–502.
17. Postic, C. & Magnuson, M. A. (2000) *Genesis* **26,** 149–150.
18. Michael, M. D., Kulkarni, R. N., Postic, C., Previs, S. F., Shulman, G. I., Magnuson, M. A. & Kahn, C. R. (2000) *Mol. Cell* **6,** 87–97.
19. Yu, J., Zhang, Y., McIlroy, J., Rordorf-Nikolic, T., Orr, G. A. & Backer, J. M. (1998) *Mol. Cell. Biol.* **18,** 1379–1387.
20. Taniguchi, C. M., Kondo, T., Sajan, M., Luo, J., Bronson, R., Asano, T., Farese, R., Cantley, L. C. & Kahn, C. R. (2006) *Cell Metab.* **3,** 343–353.
21. Cantley, L. C. & Neel, B. G. (1999) *Proc. Natl. Acad. Sci. USA* **96,** 4240–4245.
22. Cherrington, A. D. (2005) *J. Clin. Invest.* **115,** 1136–1139.
23. Lam, T. K., Pocai, A., Gutierrez-Juarez, R., Obici, S., Bryan, J., Aguilar-Bryan, L., Schwartz, G. J. & Rossetti, L. (2005) *Nat. Med.* **11,** 320–327.
24. Cai, D., Yuan, M., Frantz, D. F., Melendez, P. A., Hansen, L., Lee, J. & Shoelson, S. E. (2005) *Nat. Med.* **11,** 183–190.
25. Ueki, K., Fruman, D. A., Brachmann, S. M., Tseng, Y. H., Cantley, L. C. & Kahn, C. R. (2002) *Mol. Cell. Biol.* **22,** 965–977.
26. Inoue, G., Cheatham, B., Emkey, R. & Kahn, C. R. (1998) *J. Biol. Chem.* **273,** 11548–11555.
27. Luo, J., Field, S. J., Lee, J. Y., Engelman, J. A. & Cantley, L. C. (2005) *J. Cell Biol.* **170,** 455–464.
28. Kotelevets, L., van Hengel, J., Bruyneel, E., Mareel, M., van Roy, F. & Chastre, E. (2005) *FASEB J.* **19,** 115–117.
29. Luo, J., Sobkiw, C. L., Logsdon, N. M., Watt, J. M., Signoretti, S., O'Connell, F., Shin, E., Shim, Y., Pao, L., Neel, B. G., *et al.* (2005) *Proc. Natl. Acad. Sci. USA* **102,** 10238–10243.
30. Tran, T. T., Gupta, N., Goh, T., Naigamwalla, D., Chia, M. C., Koohestani, N., Mehrotra, S., McKeown-Eyssen, G., Giacca, A. & Bruce, W. R. (2003) *Cancer Epidemiol. Biomarkers Prev.* **12,** 47–56.
31. Taniguchi, C. M., Ueki, K. & Kahn, R. (2005) *J. Clin. Invest.* **115,** 718–727.
32. Miller, S. J., Lou, D. Y., Seldin, D. C., Lane, W. S. & Neel, B. G. (2002) *FEBS Lett.* **528,** 145–153.